Title
Minimizing and Characterizing Microplastic in Powder Material from Carpet Recycling

Author
Henderson, Alice Nicole

Publication Date
2022

Peer reviewed|Thesis/dissertation

Minimizing and Characterizing Microplastic in Powder Material from Carpet Recycling

By

ALICE NICOLE HENDERSON

THESIS

Submitted in partial satisfaction of the requirements for the degree of

MASTER OF SCIENCE

in

Agricultural and Environmental Chemistry

in the

OFFICE OF GRADUATE STUDIES

of the

UNIVERSITY OF CALIFORNIA

DAVIS

Approved:

Peter G. Green, Chair

Sanjai J. Parikh

Jenessa Gjeltema

Committee in Charge

2022

Acknowledgments:

I would like to warmly thank my thesis committee members for their time, attention, and support throughout my research and writing process. Former members of the UC Davis Environmental Soil Chemistry Lab, Dr. Devin Rippner and Jaeeun Sohng generously supported me with their time and expertise in lab at UC Davis as well as planning for and collecting data at the Lawrence Berkeley National Laboratory Advanced Light Source (LBNL ALS). Dr. Gjeltema lab student, Charlene Lujan Vega, and Dr. Swee Teh lab student, Chelsea Lam, also assisted during round-the-clock beamtime at the LBNL ALS facility. Beamline staff at the ALS, Dr. Hans Bechtel and Dr. Stephanie Gilbert Corder, were welcoming, encouraging, and incredibly knowledgeable, answering my many questions before, during and after my time at beamline 1.4. I am also grateful to California Carpet Stewardship and Dr. Robert Peoples as well as the Henry A. Jastro Research Award for providing funds to support some of my work. For additional funding and supporting my interdisciplinary interests, I am grateful to the faculty I worked with as a teaching assistant: Dr. Karen Riveles and Dr. Elizabeth Marder in the Department of Environmental Toxicology, Dr. Cort Anastasio in the Department of Land, Air and Water Resources, and Dr. Claire Goldstein in the Department of French and Italian. I am also incredibly grateful to Dr. Julia Simon in the Department of French and Italian for trusting me to teach a French class during a global disease pandemic. And finally, I'd like to thank my family and friends, especially my cohort in the Agricultural and Environmental Chemistry Graduate Group including Stephanie Arciva, Emily Steliotes, and Veronica Suarez – I quite literally could not have done this without you.

Abstract:

Mechanical deconstruction of post-consumer carpet results in plastic fibers as well as a fine powder, comprised mostly of calcium carbonate ($CaCO_{3)}$, ready for reuse. This powder is referred to as post-consumer carpet calcium carbonate (PC4) and contains low levels of microplastic fibers along with a wide range of trace components such as sand, antimony, perfluorinated compounds, and brominated flame retardants. While plastic fibers are relatively easy to reuse, the trace components of PC4 present recycling challenges. Clean-up of this powder is crucial for developing appropriate uses in recycled-content product manufacturing. Thermal treatment, ashing/combustion with oxygen present or charring/pyrolysis if oxygen is excluded, is proposed as a relatively low-cost method to break down microplastics and other hazardous components that accumulate in carpet. Fourier transform infrared (FTIR) spectroscopy was used to quantify the mass loss of polyethylene terephthalate (PET) as well as nylon 6 (N6) in PC4 samples when heated for 1 hour at 500 and 600 °C with and without oxygen. Single-bounce attenuated total reflectance, ATR-FTIR was used in addition to synchrotron-based FTIR microspectroscopy (SR-μFTIR) and a modified microscopic ATR-FTIR imaging technique using a large germanium hemisphere and focal plane array (FPA) detector. The data demonstrate that heat treatment at 600 °C successfully reduced both PET and N6 content below detection limits. Maps obtained via FTIR imaging reveal the size and spatial distribution of microplastics in PC4. This work is novel and significant as it addresses the long-term environmental challenges of waste and pollution from consumer goods and assesses the effectiveness of post-consumer carpet recycling.

Introduction:

Effective and safe waste management is a global challenge. The United Nations established 17 sustainable development goals in 2015, including the aim to ensure "sustainable consumption and production patterns," such as governments' commitment to waste prevention, reuse, and recycling (United Nations, n.d.; Walker, 2021). Another goal specifically targets plastic debris density as relates to the conservation and sustainable use of oceans. Plastic waste is a growing concern based on its ubiquity, persistence, and both documented and suspected adverse effects. Furthermore, plastic degradation in the environment when exposed to sunlight produces greenhouse gas emissions that contribute to climate change (Royer et al., 2018), among other numerous social and environmental adverse effects.

Global plastic production has increased drastically from 1.7 metric tonnes (Mt) in 1950 to 348 Mt in 2017 (Geyer, 2020). As reported in 2017, production of half of all plastic ever made occurred over the prior 13 years, from 2004 to 2017 (Geyer et al., 2017). In the US, recycling of municipal solid waste increased in recent decades from 10% in 1980 to 32% in 2018. However, this increase comes mostly from recycled paper, paperboard, and metals. Plastic made up only 4.5% of material recycled, compared to 18% of the material landfilled in 2018, second only to food waste at 24% (US EPA, 2020). Some of the most difficult materials to recycle are those made of multiple materials since the separation of various components presents both logistical and economic challenges. One such material is carpet, a common flooring material in homes, hotels and office buildings with 3.3 billion pounds discarded in the US in 2017, an estimated 10 pounds per capita (*CARE 2017 Annual Report*, 2018).

The California (CA) state government prioritized carpet recycling with Assembly Bill 2398, "Product stewardship: carpet," signed into law in 2010 and modified in 2017 with the goal of recycling 24% of post-consumer carpets by January 1, 2020 (AB 2398, 2010). According to the bill, post-consumer, discarded carpet is one of the 10 most prevalent waste materials in CA landfills, representing 3.2% (v/v) of CA municipal solid waste in 2008.

Carpet Recycling & Chemicals of Concern

In the United States, current recycling processes for post-consumer carpets result in ~60% plastic fiber and ~40% post-consumer calcium carbonate mixture known as PC4, Post-Consumer Carpet Calcium Carbonate. PC4 comes from carpet backing material which provides structure and weight to carpet. Although we strive towards a closed-loop recycling system, one where carpet can be recycled and re-sold as carpet is not currently feasible. For both mechanical and economic reasons, carpet recycling plants cannot economically remove contamination to an extent where either plastic fiber or PC4 can be used again in carpets (Peoples, 2018). However, several uses have been developed for plastic fiber including the padding that goes underneath carpets and materials for automotive, transportation, and construction industries (Peoples, 2018). The calcium carbonate powder portion (PC4) on the other hand, has a smaller number of current and potential uses. It has been considered as an agricultural soil amendment (Peoples, 2018) since calcium carbonate (lime) is often added to soils to increase pH (Carvalho & van Raij, 1997; Schreiber & Nunez, 2021); however, trace chemical components as well as microplastic in the material present concerns for use as a soil amendment.

While PC4 is principally calcium carbonate, current processing yields a product that includes roughly 10% plastic along with elevated levels of household dust contaminants. Since household

dust is known to contain a vast array of chemicals (Moschet et al., 2018) and dust accumulates in carpeting, PC4 likely contains trace chemicals at even higher levels than reported in household dust. Researchers detected 271 different chemicals in household dust samples, many of which were detected in over 50% of the 38 samples from households in the areas of Sacramento and Fresno, CA (Moschet et al., 2018). The chemicals identified include various flame retardants and polyfluorinated compounds which may have adverse human health effects and have been associated with carpet (Moschet et al., 2018; Schecter et al., 2005; Zhu et al., 2021). In particular, polybrominated diphenyl ethers (PBDEs) used as flame retardants are known trace components in PC4 as well as antimony (Sb) due to its use as a catalyst during PET plastic manufacturing (Cunningham et al., 2021). Unpublished data from Dr. Peter Green (UC Davis, Department of Civil and Environmental Engineering) indicates that perfluorinated compounds, PFCs, brominated flame retardants (BFRs), and Sb are present in PC4, and that Sb is bioavailable when applied to soil. One sample contained brominated diphenyl ether, BDE-47 and BDE-99 in the range of 3000 – 8000 ng/g. The same sample contained perfluorooctanoic acid, PFOA and perfluorooctane sulfonic acid, PFOS at 20 – 30 ng/g. Sb was measured at 8.44 mg/kg and appeared to be bioavailable to lettuce plants, accumulating in the plant roots.

Since PC4 is sieved to less than 2 mm during processing, any plastic remaining is considered microplastic, a growing environmental concern in marine as well as terrestrial environments with increasing evidence of ecosystem threats and human health concerns (de Souza Machado et al., 2019, 2020; Rainieri & Barranco, 2019; Thompson et al., 2004). Removing microplastic is a crucial step before commercial use of PC4.

Microplastic as an Environmental Hazard

Microplastics are often defined as any plastic particle < 5 mm in size, however a recent report from the European Chemicals Agency proposed a more detailed definition, including particles with dimensions ranging from 1 nm to 5 mm, fiber lengths ranging from 3 nm to 15 mm, and a length-to-diameter ratio > 3 (ECHA, 2019). Plastic particles < 1 nm are increasingly referred to as nanoplastics and have greater potential than larger particles to cross membranes such as the blood-brain barrier and the human placenta (de Souza Machado et al., 2018).

While the hazards of microplastic in marine environments have received substantial study as early as 1972 (Carpenter & Smith, 1972; Wong et al., 1974), a more recent body of work investigates microplastics as a threat to terrestrial ecosystems (de Souza Machado et al., 2018; Rillig, 2012, 2018). This work is especially important to consider regarding possible agricultural use of post-consumer material such as PC4. Nizzeto et al. 2016 reported an annual accumulation of > 300,000 tons of microplastic in farmland globally, and the amount of microplastic particles on land may be 4 to 23 times more abundant than in the ocean (de Souza Machado et al., 2018; Nizzetto et al., 2016). It has been established that application of sewage sludge containing microplastic to agricultural soils is a direct source of microplastics in the terrestrial environment (Corradini et al., 2019; Mahon et al., 2017; Wang et al., 2019). Based on mounting evidence of microplastic's environmental and toxicological threats, widespread application of other waste materials containing microplastic to agricultural soils is not advisable.

Once in the environment, a growing body of research suggests that microplastics interact with biota, geochemical and biophysical processes, likely causing toxic effects in the environment (de Souza Machado et al., 2018). Our understanding of microplastic effects on the environment includes their effects in conjunction with other pollutants, and the effects of microplastic particles themselves (Wang et al., 2019). Microplastics are found in a wide range of polymer

types, sizes, and shapes. They often contain chemicals added intentionally during manufacturing such as plasticizers and metals which can leach from microplastics to the environment or within organisms. Microplastics can adsorb organic pollutants, metals, and antibiotics from their environment which could pose a significant environmental threat (Brennecke et al., 2016; Li et al., 2018; Teuten et al., 2007). Regarding microplastic particles themselves, nanoplastics (< 1 μm) can interact with biological membranes, molecules, and organelles (de Souza Machado et al., 2018). Specific microplastics could affect key soil properties including water holding capacity, bulk density, microbial activity, and soil structure and function (de Souza Machado et al., 2018).

Microplastic pollution has gained attention from the United Nations (UNEP, 2016) as well as the European Union (European Union, 2017). In the US, California passed Senate Bill, SB 1422, and SB 1263 in 2018 to address microplastic concerns. SB 1422, "California Safe Drinking Water Act: Microplastics," requires the State Water Resources Control Board to adopt a definition of microplastics in drinking water as well as a standard methodology to test microplastic levels in drinking water and to test and report microplastic levels in CA drinking water to the public for four years (SB 1422, 2018). Also passed in 2018, SB 1263, "Ocean Protection Council: Statewide Microplastics Strategy," targets marine microplastics and requires that the Ocean Protection Council develop a prioritized, detailed research plan in support of developing risk assessments for microplastics in marine habitats (SB 1263, 2018). While the direct hazards to humans through microplastic in air, water and food products are uncertain, there is a growing concern for human exposure via indoor and outdoor air inhalation ingestion of certain foods (Gaston et al., 2020; Rainieri & Barranco, 2019).

Microplastic & Pyrolysis

To remove microplastic from PC4 for developing uses of this post-consumer carpet material, we hypothesize that thermal treatment of carpet powder will be an effective and relatively low-cost method to minimize microplastic content. Pyrolysis has been studied in the context of microplastic mitigation in sewage sludge, a large source of microplastic in the environment (Ni et al., 2020). Recent data shows that pyrolysis temperatures as low as 450 °C decomposed 99.7% of microplastic particles of low density, density < 1.1 g/cm^3, in sewage sludge (Ni et al., 2020). In recent years, pyrolysis has gained much attention due to its use in the production of biochar. The term "biochar" refers to a wide range of pyrolyzed biomass feedstocks including wood, orange peels, nutshells, manure and sewage sludge with potential in certain cases to benefit agricultural production, climate change mitigation and soil contaminant remediation (Gelardi & Parikh, 2021; Mukome et al., 2013). For the treatment of sewage sludge, it is suggested that pyrolysis (oxygen excluded) may be superior to incineration (oxygen present) since incineration may produce more harmful emissions such as furans and dioxins (Ni et al., 2020). Temperatures above 450 °C are crucial since lower pyrolysis temperatures can produce new polymers through reactions between microplastic particles and other organics. Microplastics may also combine with heavy metals and more readily adsorb other contaminants as their surfaces become rough with low-temperature treatment (Ni et al., 2020). We have tested temperature treatments at 500 °C and 600 °C both with and without oxygen present to determine which may be more appropriate to remove microplastic and other hazardous components from PC4 before reuse.

Measuring Microplastic

Developing standardized methods for measuring microplastic is essential to supporting CA, national and global policy agendas regarding monitoring and mitigation of microplastic in the

environment. Challenges associated with measuring microplastics in the environment include the complexity of the sample matrix such as soil and biota or tissues as well as the diversity of microplastic particles and adhered components. The term “microplastic” encompasses a wide range of particle sizes, polymer types, shapes, chemical additives, sorbed contaminants, and states of aging (Ivleva, 2021). The sheer number of recent review papers describing analytical methods for microplastic analysis shows how quickly methods are developing as concerns and policies around this widespread environmental contaminant increase (Bläsing & Amelung, 2018; Brennecke et al., 2016; He et al., 2018; Hidalgo-Ruz et al., 2012; Huppertsberg & Knepper, 2018; Ivleva, 2021; Primpke et al., 2020; Shim et al., 2017a; Silva et al., 2018; Song et al., 2015).

Analytical techniques for identifying and quantifying microplastic include methods for physical characterization such as microscopy and methods for chemical characterization including spectroscopy and thermal analysis (Shim et al., 2017a). Methods for chemical analysis can be further generalized as mass-based methods which include thermal degradation combined with gas chromatography/mass spectroscopy (GS/MS) and nondestructive, particle-based methods including various types of vibrational spectroscopy, especially Fourier transform infrared (FTIR) and Raman spectroscopies (Shim et al., 2017a). FTIR spectroscopy has been used since some of the earliest analytical research measuring microplastic while Raman spectroscopy has grown in popularity more recently, especially for the analysis of very small (< 1 mm) microplastics. Combined with an optical microscope, μ-Raman has been recommended for particles smaller than 10-20 μm while μ-FTIR can be preferred for particles smaller than 500 μm (Ivleva, 2021). In general, FTIR and Raman are complementary methods for particles >20 μm depending on the specific research questions asked and project needs (Käppler et al., 2016).

While visual identification remains incredibly common, FTIR and Raman spectroscopies are increasingly used to achieve more accurate and definitive identification and quantification of plastic particles. They are often combined with microscopy, typically to identify discrete plastic particles and then quantify microplastic via extrapolation to determine the number of particles per volume or mass of environmental sample including atmospheric fallout, soil, beach sediment, and water (Browne et al., 2010; Cabernard et al., 2018; Cai et al., 2017; Enders et al., 2015; Scheurer & Bigalke, 2018; Zhou et al., 2018).

Attenuated Total Reflectance - FTIR Spectroscopy

We have used attenuated total reflectance (ATR) FTIR spectroscopy to analyze a variety of PC4 samples and identify absorbance bands corresponding with plastic polymer standards which are

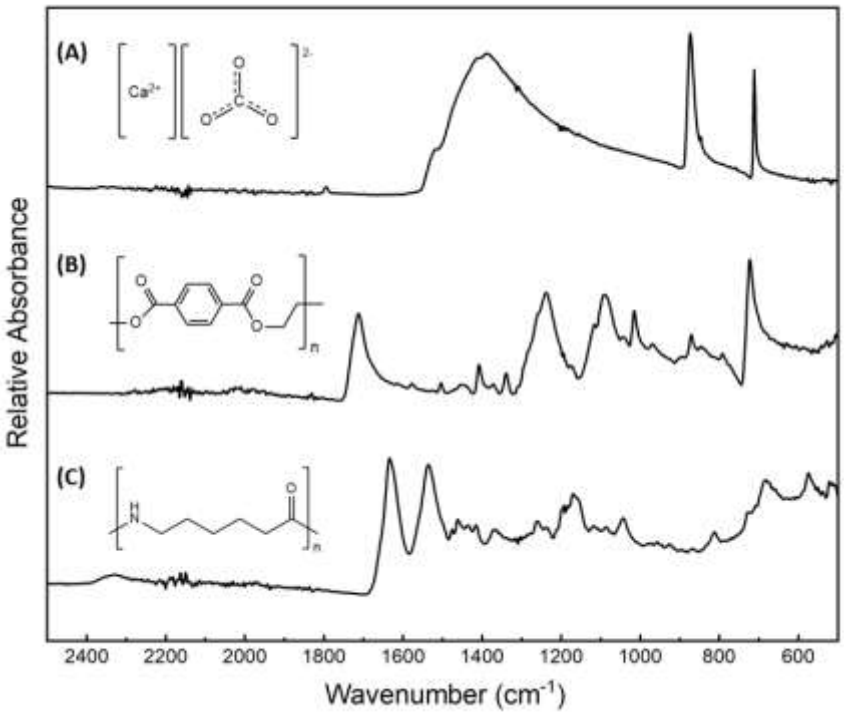

Figure 1: Chemical structures and FTIR spectra of components likely present in PC4: (A) $CaCO_3$, (B) PET, and (C) N-6.

known or suspected in PC4. Figures 1 and 2 show FTIR spectra and chemical structures for components we expected to find in PC4: calcium carbonate ($CaCO_3$), polyethylene terephthalate (PET), nylon-6 (N-6), polystyrene latex (PS), polypropylene (PP), and polyethylene (PE).

The FTIR spectra show the relative absorbance of infrared light based on vibrational characteristics of molecular bonds, or functional groups. Only chemical bonds with a dipole moment are detectable via FTIR and the magnitude of IR radiation absorbed increases the amplitude of bond vibration (Pavia et al., 2015). In this study, spectra are illustrated with wavenumber (cm^{-1}) as the unit of energy of infrared radiation and absorbance as the value of the intensity of signal measured. As described by the Beer-Lambert-Bouguer law, absorbance is proportional to sample concentration, layer thickness, and molar attenuation coefficient (Rocha-Santos & Duarte, 2017). ATR is a rapid, surface analysis method common for microplastic

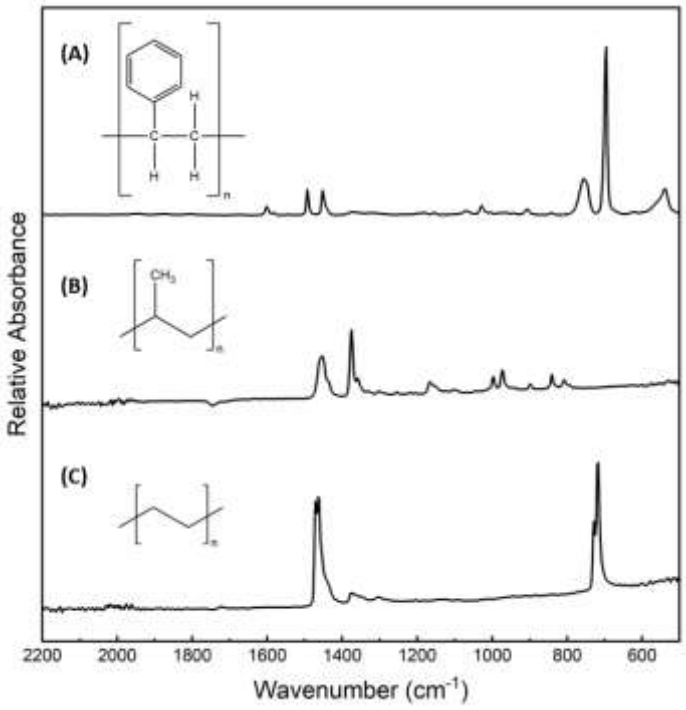

Figure 2: Chemical structures and FTIR spectra of components likely present in PC4: (A) PS latex, (B) PP, and (C) PE.

analysis for particles down to 2mm (Rocha-Santos & Duarte, 2017). While transmission FTIR often requires sample material to be finely ground and dispersed at low concentration in a KBr pellet to show a good linear correlation with concentration (Chen et al., 2014), ATR requires minimal sample preparation due to the low penetration depth of the IR beam (about 0.5 to 2μm). This low penetration depth minimizes the overloading of vibrational bands as well as minimizing the effects of residual moisture (Rocha-Santos & Duarte, 2017).

FTIR Microspectroscopy and Chemical Imaging

While many environmental samples contain microplastic pieces large and distinct enough to be easily identified as plastic by the naked eye or optical microscope, these techniques have been demonstrated to underestimate the total microplastic particles (Lenz et al., 2015). Identifying polymer type for particles one at a time can be prohibitively costly and time consuming. Furthermore, it is well established that plastic particles exist at sizes much too small to be individually handled for analysis (Primpke et al., 2020). For particles > 10 – 20 μm, micro-FTIR spectroscopy (μ-FTIR) combines an optical microscope with an FTIR spectrometer which can perform automated analysis of preselected particles on a filter surface, or of the filter surface indiscriminately (Ivleva, 2021). While collecting spectra across an entire filter surface is time-consuming, spectra can instead be collected from a representative subarea such as 0.2 - 6% of the total filtered surface, 2 - 4 mm^2 areas on a 47 mm diameter filter or membrane (Corami et al., 2020; Harrison et al., 2012; Vianello et al., 2013). In addition, focal plane array (FPA) detectors allow for time-efficient μ-FTIR analysis of a large filter area since multiple detectors are arranged in an array and collect spectra simultaneously. This enables hyperspectral imaging, a record of a three-dimensional hypercube with a combination of spatial and spectral information.

Hyperspectral imaging techniques are increasingly used for analyzing an entire filter surface in a time-efficient manner. These techniques have been used to detect microplastic in soil, seawater, wastewater and the intestinal tracts of fish (Shan et al., 2018, 2019; Tagg et al., 2015; Y. Zhang et al., 2019). Preprogrammed and semi-automatic mapping without preselection of particles for analysis reduces the manual effort required for FTIR analysis and the use of a focal plane array (FPA)-based reflectance imaging methods enables mapping of 150 – 250 μm sized particles across larger areas, such as a filter surface relatively quickly and without compromising spatial resolution compared to more traditional single-beam mapping (Tagg et al., 2015). For example, an FPA detector with 64 x 64 detector elements combined with a 15x IR objective lens facilitates measurement of 4096 spectra simultaneously with each measurement on an area of 170 x 170 μm, or a pixel resolution of 2.7 μm (Löder et al., 2015). Scans of 47 mm membrane filters have been completed in under 9h with one scan per pixel and under 16 h with 2 scans per pixel (Tagg et al., 2015).

Measuring Microplastic in PC4

Unlike most environmental samples with complex matrices, we can detect microplastic within PC4 via direct measurements of bulk samples due to the relative homogeneity of the material, ~90% calcium carbonate. However, standard FTIR spectroscopy cannot reveal chemical features of all microplastics since the diameter of the IR beam aperture limits detection to particles 10 μm and larger (Shim et al., 2017a) and microplastics are known to exist below this size. In practice, microplastics below 50 μm in length can be difficult to identify accurately by FTIR (Shim et al., 2017a). Synchrotron-based FTIR (SR-FTIR) microspectroscopy is advantageous for microplastic analysis since better spatial resolution (approximately 1 μm) can be achieved (Bancin et al.,

2019; Kunz et al., 2016). SR-FTIR microspectroscopy provides higher accuracy and precision, provides very good signal-to-noise ratios, can allow faster data collection depending on the measurement objective, and reaches diffraction limits as small as a few micrometers with ultrahigh spatial resolutions (Yu et al., 2004).

In this study, we used a combination of ATR-FTIR, SR-μFTIR and FPA-based μFTIR hyperspectral imaging (FTIR imaging) to test a range of thermal treatments to determine which are most promising for reducing the plastic content of PC4 samples from CA carpet recyclers. Thermal treatments include ashing/combustion with oxygen present as well as charring/pyrolysis under pure nitrogen gas within a furnace. We hypothesize that furnace treatment of PC4 will decrease the plastic content, resulting in a product more amenable for commercial use, such as low-grade concrete. Our objectives included investigating the relative benefits and drawbacks of three FTIR methods, benchtop ATR-FTIR, SR-μFTIR and FTIR imaging for analyzing the plastic contents of PC4. The analysis objectives were to describe the microplastic content of PC4 including mass percent, spatial distribution, and approximate size of PET and N6 particles. Finally, we aimed to determine whether ashing and charring at 500 and 600 °C can effectively remove microplastic from PC4.

Materials and Methods:

Chemicals and Equipment

Post-consumer carpet calcium carbonate (PC4) samples were obtained from two, CA carpet recycling facilities, referred to as facility "B" and facility "C." PC4 from facility B was collected in 2017 and PC4 from facility C was collected in 2017 as well as 2019, after significant changes to mechanical processing. Nylon-6 powder (N6, 55 µm) and polyethylene terephthalate (PET, 300 µm) plastic standards were purchased from Goodfellow (Huntington, England). Polystyrene latex dry microspheres (PS latex, 1 µm) and polyethylene powder, low density (PE, 500 µm) were purchased from Alfa Aesar (Ward Hill, MA). Calcium carbonate standard, 99+%, was purchased from ACROS Organics (New Jersey, USA). Heat treatments were performed using a Thermolyne type 6000 furnace. Fourier transform infrared (FTIR) attenuated total reflectance (ATR) spectra were collected using a Nicolet 6700 FTIR (Thermo Scientific, Waltham, MA), a deuterated triglycine sulfate (DTGS) detector, and a single-bounce diamond crystal. Synchrotron-based FTIR microspectroscopy (SR-µFTIR) and FPA-based FTIR hyperspectral imaging (FTIR imaging) were conducted at the Lawrence Berkeley National Laboratory Advanced Light Source on beamlines 1.4.3 and 2.4.2 (Berkeley, CA).

Heat treatment

Approximately 10 g of PC4 was heated in porcelain crucibles (Fisher, Pittsburgh, PA) for each sample evaluation. After loading samples, the furnace was heated to the desired temperature and held for 1 h. For our 500 °C treatment, samples were heated for a total of 2.5 h with a 1 h hold from 480-500 °C. Initial 600 °C treatment, samples were heated for a total of 4 to 7 h with a 1 h

hold from 580-620 °C (Supplementary Data Appendix, Table 1). Ash samples were created in the presence of oxygen while char samples were made using a nitrogen generator to purge oxygen from the furnace for pyrolysis. ATR-FTIR spectra were taken of each sample before and after heat treatment and samples were stored in 50mL polypropylene centrifuge tubes with plug caps, VWR (Radnor, PA). Pure calcium carbonate was also stored in the same type of centrifuge tube and spectra were taken to determine whether detectable plastic from sample tubes could contaminate samples to a detectable degree.

ATR-FTIR Spectroscopy

Spectra were collected on a Nicolet 6700 spectrometer using a Pike Technologies (Madison, WI) GladiATR accessory for all control PC4 samples and char trials. ATR spectra were collected with a DTGS detector and single-bounce diamond crystal internal reflective element (IRE) with 256 co-averaged scans per spectrum at a resolution of 4 cm^{-1}.

Concentrating Microplastic Samples

To concentrate the microplastic in PC4 samples, $CaCO_3$ was removed via reaction with a 2% HCl solution. Past studies have used dilute HCl from 5% (Bancin et al., 2019) up to 20% (Nuelle et al., 2014) to concentrate microplastic samples without impacting the size, shape, or quantity of PET or N6 particles. For our purposes, 2% HCl was sufficient to remove $CaCO_3$. Four mL of 2% HCl was added to 50 mg of unheated PC4, ash, or char, as well as a control flask with pure $CaCO_3$, in a 25 mL Erlenmeyer flask, swirled for 1 min and left on the benchtop covered with a Kimwipe (Kimberly-Clark, Irving, TX) to allow for gas exchange for 72 h, swirling by hand for 1 min approximately every 24 h. After 72 h, an additional 2 mL of HCl was added after which no

white particles were visible in the flask initially containing pure $CaCO_3$. The concentrated sample was then collected on polytetrafluoroethylene (PTFE) laminated membrane filters (GE, Boston, MA) and dried on closed PetriSlides™ (Fisher, Pittsburgh, PA) in a desiccator for 72 h. ATR-FTIR spectra of samples were taken directly from the filter since material remaining from ash and char samples was too fine to remove. Filters were overturned on the diamond ATR crystal and measured approximately midway between the center and edge of collected material.

Plastic Quantification by FTIR Spectra and Standard Curve

Since carpet recycling facilities track the type of carpet fiber plastic they process, we were able to perform target analysis for PET and N6 fibers. Standard mixtures of $CaCO_3$ and plastic powder were prepared at 1, 2, 5, 10, 15 and 20% by mass. Calibration curves were constructed for PET and N6 in $CaCO_3$ using peak height values of diagnostic peaks of each plastic with minimal overlap with other PC4 components including $CaCO_3$ and latex. For PET this was the peak height around 1712 cm^{-1}, and for N6, this was the peak height maximum around 1633 cm^{-1} (Figure 3).

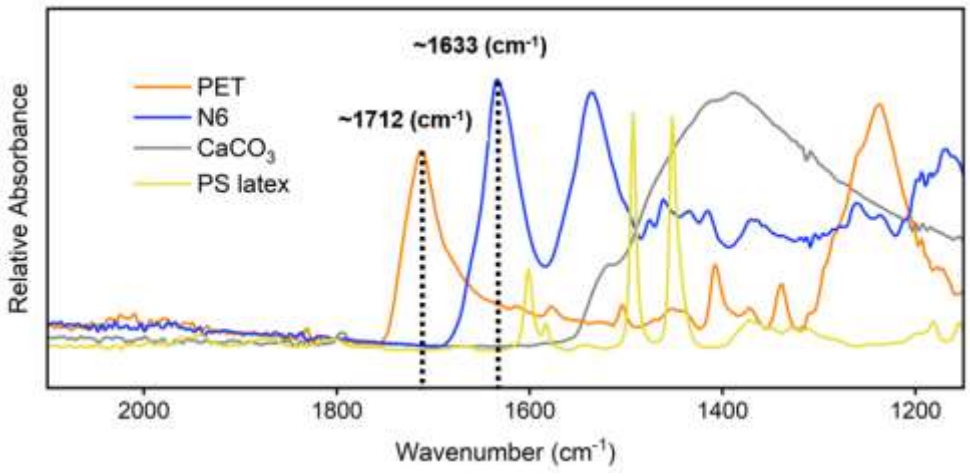

Figure 3: Spectra for standard components quantified in PC4, N6 and PET, with diagnostic peaks indicated at 1633 and 1712 cm^{-1}, along with components that have nearby and overlapping absorbance bands ($CaCO_3$ and PS latex).

Peak height was measured from a horizontal baseline set at the left side edge of the chosen peak. For PC4 samples, peak heights for PET and N6 were measured from the same baseline. Peak height values were measured using OMNIC software (Thermo Scientific, v. 9.8.286, Waltham, MA). Calibration curves were developed using MS Excel and were highly linear (R^2= 0.95 for Nylon-6 and R^2= 0.98 for PET). Calibration curves were used to quantify mass % PET and N6 in unheated PC4, ash and char samples. This calculation was performed with both concentrated samples without $CaCO_3$ and unconcentrated samples containing $CaCO_3$.

SR-based FTIR Microspectroscopy

To attain micro-scale maps of plastic particles within the PC4 mixtures, microspectroscopy instrumentation was used at the Lawrence Berkeley National Lab Advanced Light Source. Beamline 1.4 has a synchrotron (SR) light source and interferometer resolution up to 0.125 cm^{-1}. The sample was sprinkled onto a gold-plated slide (Platypus Technologies, Madison, WI) with excess sample removed by gently tapping the slide in a vertical position so that individual particles could be identified under the microscope. Particles were analyzed in reflectance mode with a KBr beam splitter and a mercury, cadmium, telluride (MCT) detector. Reflectance spectra were recorded from 4000 to 650 cm^{-1} with 36 co-averaged scans at a 4 cm^{-1} resolution. Twenty maps of individual particles from unheated PC4 sample C19 were created to investigate the size variation and distribution of microplastics within the samples.

Since using reflectance mode to analyze individual particles produces spectra susceptible to the variations in sample surface conditions (Song et al., 2015), we also used a modified microscopic ATR technique utilizing a large Ge hemisphere to compress our sample and improve spatial resolution based on the high index of refraction of the hemisphere (~4).

Focal plane array-based µFTIR imaging

ATR-FTIR microspectroscopy was used with a large-radius germanium hemispherical crystal as the IRE. The Ge hemisphere compressed samples for better spectral results in reflectance mode and had the added benefit of increasing the numeric aperture of imaging and improving spectral resolution by a factor of 4 due to the high index of refraction of Ge (~4). This modified µFTIR imaging technique was coupled with a high-density focal plane array detector (FPA), allowing for spectral images with dimensions from 100 – 900 µm and spatial resolution approaching 1 µm (Hao et al., 2018). Beamline 2.4.2 has an internal globar light source, a 700 µm field of view, and a diffraction-limited spot size.

Image Processing and Component Classification

Hyperspectral data from micro-FTIR imaging were processed and analyzed using Quasar software (University of Ljubljana, Slovenia, v. 1.2.1). Spectra preprocessing steps involved cutting spectra to a range of 1200 – 2000 cm^{-1}, smoothing spectra using the Savitsky-Golay filter with 21 points of smoothing, obtaining the polynomial order 2 and 2^{nd} derivative, rubber band baseline correction and vector normalization. Spectra were then classified using k-means clustering and cluster assignments were used to color hyperspectral images to show the spatial distribution of key components. Silhouette scores were used to determine an appropriate number of components (Supplementary Data Appendix, Table 2) and exploration of the individual spectra the regions identified with k-means clustering area were used to determine the identity of components.

Results:

Microplastic in PC4

After removing calcium carbonate ($CaCO_3$), we identified polyethylene terephthalate (PET) and nylon 6 (N6) with high certainty as well as polypropylene (PP) and polystyrene latex (PS latex). Figure 4 shows the ATR-FTIR spectra of unheated PC4 after $CaCO_3$ removal in the region where peaks are most clearly distinguishable (1800 – 1200 cm^{-1}). Samples B17 and C19 contain both PET and N6, whereas, for C17, only PP was detected in the IR spectrum. Sample C17 contained the largest amount of visibly distinguishable fibers, some up to 1 cm in length, distinctly colored red, pale blue, and black. Their chemical identity was confirmed by separating

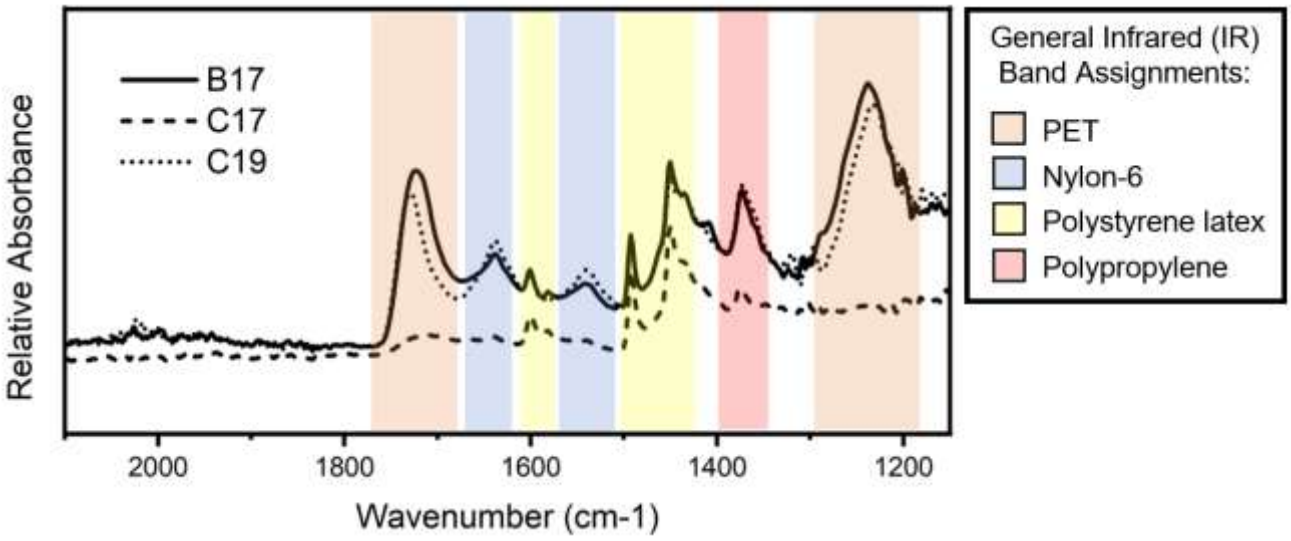

Figure 1: ATR-FTIR spectra of unheated PC4 with $CaCO_3$ removed. General infrared band assignments are shown for polymers expected to be in PC4.

suspected plastic fibers with tweezers and collecting an IR spectrum of 20 to 30 fibers. These spectra were compared with spectra of polymer standards, confirming that most of the visible fibers in C18 are PP (Supplementary Data Appendix, Figure 1).

Sr-μFTIR in reflectance mode can cause spectral interference due to the rough particle surfaces when analyzing discrete particles. Although individual particles were mapped, the spectra were difficult to interpret due to this interference. Using an FPA camera, larger maps were obtained (176 μm x 176 μm in 8 minutes), although without the SR light source. Figure 5 shows, for

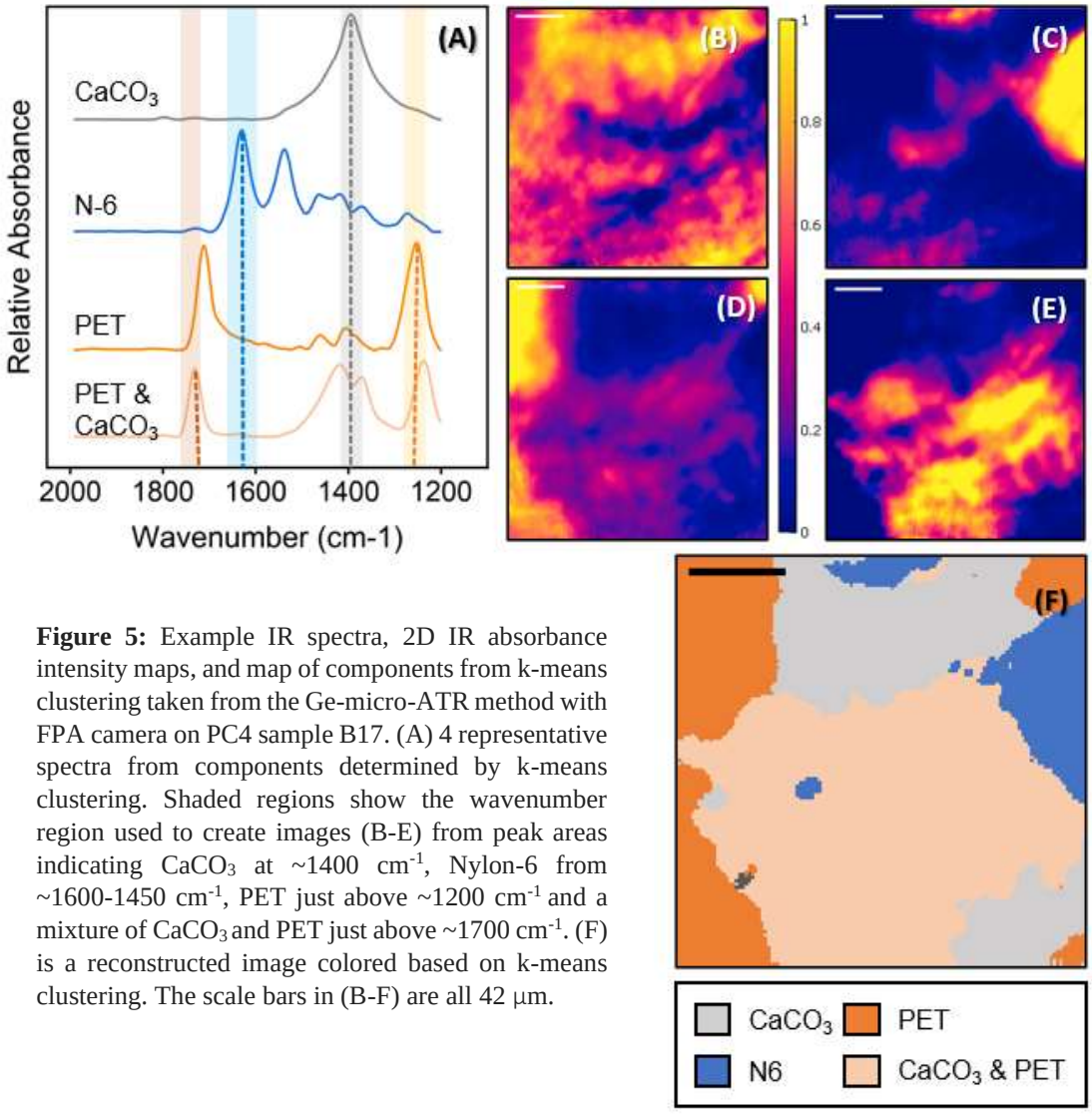

Figure 5: Example IR spectra, 2D IR absorbance intensity maps, and map of components from k-means clustering taken from the Ge-micro-ATR method with FPA camera on PC4 sample B17. (A) 4 representative spectra from components determined by k-means clustering. Shaded regions show the wavenumber region used to create images (B-E) from peak areas indicating $CaCO_3$ at ~1400 cm^{-1}, Nylon-6 from ~1600-1450 cm^{-1}, PET just above ~1200 cm^{-1} and a mixture of $CaCO_3$ and PET just above ~1700 cm^{-1}. (F) is a reconstructed image colored based on k-means clustering. The scale bars in (B-F) are all 42 μm.

unheated PC4 sample B17, representative FTIR spectra (Figure 5A) and 2D IR absorbance intensity maps of the highlighted regions corresponding to the components from k-means clustering, identified as $CaCO_3$, N6, PET, and a mixture of PET and $CaCO_3$ (Figure 8B-E).

Figure 8F shows the result of k-means clustering with four components. The shapes of the components displayed in Figure 8F correspond with the shapes in the maps of individual components, Figure 8B-E. Additional examples of k-means clustering with unheated PC4 are shown in Supplementary Data Appendix Figures 2 and 3.

Heat Treatment of PC4

Heating samples of post-consumer calcium carbonate (PC4) resulted in sample mass loss of 18 to 25% at 500 °C, 21 to 32% at 600 °C, and 22 to 35% at 680 °C for samples tested from two different carpet recycling facilities (Supplementary Data Appendix Table 3). Comparing 500 and 600 °C, % mass loss increased by 3-5% for the higher temperature. The mass loss increased a small amount (1-3%) when temperature treatment was increased to 680 °C. Photos of ash and char samples along with unheated samples are shown on filters after removing $CaCO_3$ in Supplementary Data Appendix Figure 4. Upon heat treatment, colored fibers were no longer visible in ash and char and the material turned from a pale beige to darker gray or black.

ATR-FTIR spectra reveal the altered chemical composition of PC4 sample B17 upon heat treatment at 500 and 600 °C (Figure 6). Spectra of PC4 after heating at 600 °C closely resemble the spectrum of calcium carbonate ($CaCO_3$), the primary, component of PC4. However, spectra of unheated PC4 and PC4 heated at 500 °C contain other peaks in the fingerprint region (600 – 1400 cm^{-1}) as well as the region between roughly 1500 cm^{-1} and 1800 cm^{-1}.

After removing $CaCO_3$ from PC4 samples, spectra were less obscured and additional PC4 components were identified. Figure 7 shows the spectra of filters with concentrated non-$CaCO_3$ components of PC4 both unheated and after heating at 500 and 600 °C. Figure 8 presents the spectra for PC4 ash and char samples on PTFE filters after $CaCO_3$ removal.

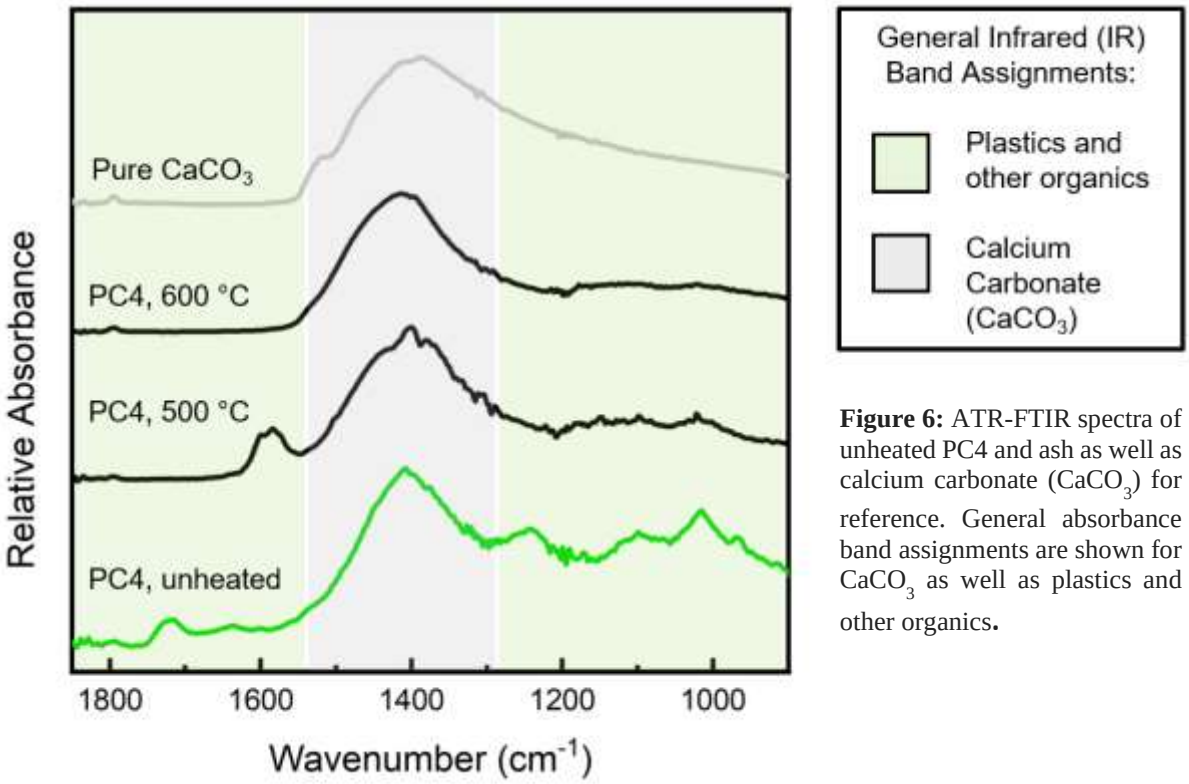

Figure 6: ATR-FTIR spectra of unheated PC4 and ash as well as calcium carbonate ($CaCO_3$) for reference. General absorbance band assignments are shown for $CaCO_3$ as well as plastics and other organics**.**

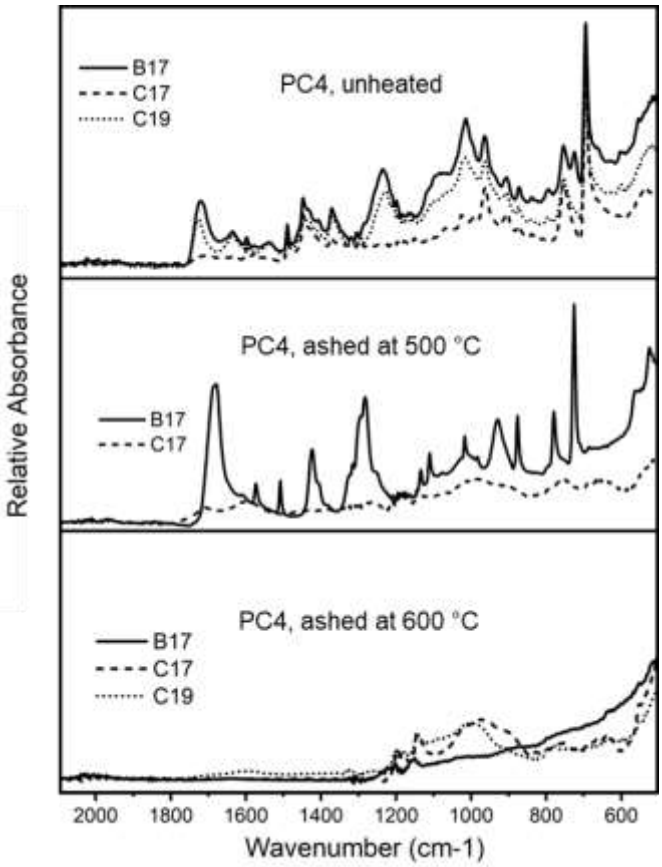

Figure 7: ATR-FTIR spectra of unheated PC4 and PC4 ashed at 500 and 600 °C with $CaCO_3$ removed.

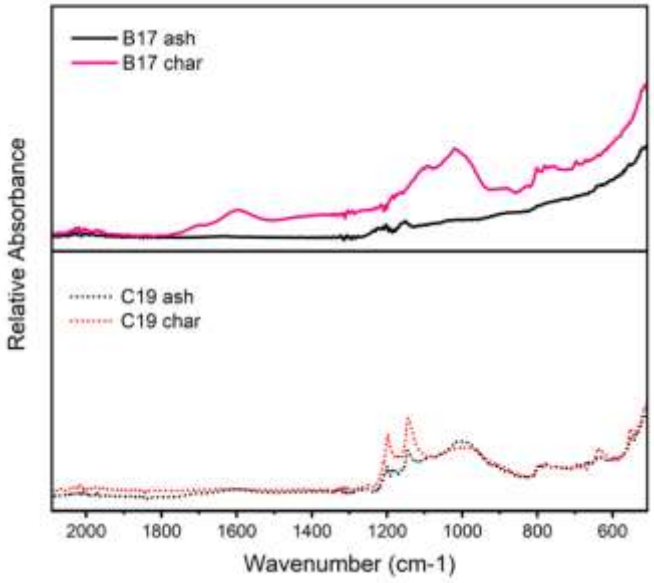

Figure 8: ATR-FTIR spectra of PC4 ash and char samples after CaCO3 was removed from samples B17 and C19.

Table 1 provides the quantification results from spectra before $CaCO_3$ removal while Table 2 shows quantification results after $CaCO_3$ removal. Before removing $CaCO_3$, PC4 was found to contain 17 to 18% plastic by mass (6-7% N6 and 11-12% for PET). After removing $CaCO_3$, PC4 was found to contain at least 3% but up to 15% plastic by mass (1-4% N6 and 2-11% PET). C17 had no measurable peaks for N6 or PET before $CaCO_3$ was removed; however, small peaks were observed and quantified after $CaCO_3$ removal, improving detection limits. Quantified plastic for sample B17 only decreased from 6 to 4% of N6 mass. On the other hand, sample C19, which was quantified at 18% total plastic in untreated PC4, dropped to just 8% total plastic after removing $CaCO_3$. N6 and PET were below detection limits for ash and char treatments at both 500 and 600 °C.

Table 1: Quantification of N6, PET and total plastic via calibration curves and spectra from unheated PC4, ash, and char samples including $CaCO_3$.

Sample	%mass N6	%mass PET	Total %mass plastic
B17	6	11	17
B17, 500 °C	< 1	< 2	< 3
B17, 600 °C	< 1	< 2	< 3
B17, 600 °C, without O_2	< 1	< 2	< 3
C17	< 1	< 2	< 3
C17, 500 °C	< 1	< 2	< 3
C17, 600 °C	< 1	< 2	< 3
C19	7	12	18
C19, 600 °C	< 1	< 2	< 3
C19, 600 °C, without O_2	< 1	< 2	< 3

Table 2: Quantification of N6, PET and total plastic via calibration curves and spectra from unheated PC4 samples, ash and char with $CaCO_3$ chemically removed.

Sample	%mass N6	%mass PET	Total %mass plastic
B17	4	11	15
B17, 500 °C	<0.15	<0.29	<0.44
B17, 600 °C	<0.09	<0.18	<0.27
B17, 600 °C, without O_2	<0.10	<0.20	<0.30
C17	1	2	3
C17, 500 °C	<0.03	<0.06	<0.09
C17, 600 °C	<0.02	<0.05	<0.07
C19	2	6	8
C19, 600 °C	<0.04	<0.09	<0.13
C19, 600 °C, without O_2	<0.04	<0.08	<0.12

Discussion:

Relative Merits of Instrumental Methods

Environmental microplastics present challenges for analytical measurement common among toxicants including low concentrations and complex sample matrices. Microplastic analyses also come with unique challenges stemming from the broad diversity of materials encompassed by this general term. Microplastics themselves are diverse in their size (from 5 mm to 1 µm), polymer type, shape (including fibers, spheres, films, and foams), chemical additives, sorbed contaminants, aging state, and degree of weathering (Ivleva, 2021; Shim et al., 2017b). In contrast, microplastics in PC4 from carpet recycling facilities are in relatively high concentration and have a somewhat homogenous sample matrix – primarily $CaCO_3$. Furthermore, since microplastics in PC4 are from deconstructed carpet, the majority of microplastics are of similar polymer type and shape (thin fibers). Synthetic carpets in the US are made from plastic fibers made of nylon (e.g. N6), polypropylene (PP), polyester (PE), polyethylene terephthalate (PET) or a mixture (Sotayo et al., 2015). Furthermore, PC4 microplastics have negligible weathering from the sun or other environmental exposure since carpet is made from virgin polymer and primarily used indoors, although foot traffic introduces mechanical weathering. While carpet likely comes in contact with a wide array of organic compounds and chemical contaminants (Moschet et al., 2018) that could sorb to its fibers, these compounds are not present in PC4 at high enough concentrations to present challenges for FTIR analysis of microplastic in PC4.

While non-target analysis is necessary to assess microplastic in most environmental samples, due to the nature of PC4 and carpet recycling facilities' ability to track what type of polymer carpets they process, we can perform target analysis for known microplastic components (PET and N6).

Units representing the number of particles made sense early in microplastic analysis when identification was frequently made by visual identification of individual particles (often confirmed via spectroscopy). Today, however, methods have progressed to include mass-related quantification methods such as high-pressure fluid extraction (Fuller & Gautam, 2016) and pyrolysis-gas chromatography-mass spectrometry with thermochemolysis (Fischer & Scholz-Böttcher, 2017). Although researchers still frequently use FTIR spectroscopy for particle-related quantification, we present a method for using FTIR spectroscopy to analyze samples and determine plastic concentrations using plastic standards to create calibration curves in terms of mass % plastic microspheres in pure $CaCO_3$. While similar methods have been used to quantify minerals in carbonate rock (Henry et al., 2017), chemical components of sorghum grain (Lin et al., 2021), and sugars in honey (Anjos et al., 2015), it is not common for microplastic analysis where environmental matrices are usually too complex. Since PC4 is composed primarily of $CaCO_3$, we can use calibration curves for plastic standards mixed with $CaCO_3$ to quantify certain plastic components.

While PET and N6 were initially quantified from spectra including $CaCO_3$, we determined that 2% HCl, was sufficient to remove $CaCO_3$ and concentrate microplastic particles for improved instrument detection. It is unlikely this low concentration had any effect on PET and N6 particles. PS latex and PP were also minimally affected at this level since peaks for both polymers remain unchanged (Figure 1). Detection limits for N6 and PET improved from 1% and 2% respectively (Table 1), to below 0.15% for N6 and below 0.44% for PET.

When reporting microplastic data, it is useful to include both concentration and particle size since these variables have distinct toxicological implications and can vary independently from each other. Although μFTIR imaging was not effective for quantitative analysis in this study,

qualitative analysis yielded information about size distribution as well as polymer types. This technique may also be quantitatively relevant for PC4 microplastic; however, $CaCO_3$ removal and additional method refinement are necessary since, for standard mixtures of $CaCO_3$ with plastic microspheres, detection limits were relatively high for μFTIR imaging, approximately 10% for N6 and 20% for PET. Similar hyperspectral imaging instrumentation has been used to analyze microplastic particles between 100 and 1000 μm, however these were individual particles collected on a filter material after initial sample preparation such as visual identification or peroxide treatment to remove biogenic or other non-plastic material (Faltynkova et al., 2021). Despite challenges involving sample preparation to concentrate microplastics and striking a balance between amount of data collected, measurement times and imaging quality, hyperspectral imaging techniques are advantageous primarily due to the speed of spectral acquisition (Faltynkova et al., 2021).

Microplastics in PC4

FTIR spectra of PC4 samples revealed both N6 and PET plastics with peaks between 1500 and 1800 cm^{-1} (Figure 6). While N6 and PET were relatively distinguishable from $CaCO_3$, other polymers such as PP and PS latex are difficult to discern without first chemically removing $CaCO_3$ (Figures 3 and 4). Although PC4 sample C17 did not contain any peaks characteristic of N6 or PET, spectra after chemically removing $CaCO_3$ revealed the presence of both PS latex and PP. A spectrum of a portion of 20 to 30 fibers selected by hand from C17 showed a strong match with our PP standard spectrum (Supplementary Data Appendix, Figure 1). With $CaCO_3$ chemically removed, PP and PS latex were detected in both B17 and C19 as well as C17. While we developed quantification methods for N6 and PET based on initial spectra of PC4 with

$CaCO_3$ obscuring much of the spectral detail, we only qualitatively identified other plastics, PP and PS latex (Figure 1).

Based on the % mass of samples remaining after HCl treatment (Supplementary Data Appendix, Table 4), we expected the total amount of plastic in unheated PC4 to be below 27% for B17, below 15% for C17, and below 18% for C19. Before removing $CaCO_3$ (Table 1), the total % mass of N6 and PET was 17% for B17, 18% for C19, and below detection limits for C17. This value for C19 is too high based on the % sample mass remaining after HCl treatment. After HCl treatment (Table 2), the total % mass of N6 and PET was 15% for sample B17, 3% for sample C17, and only 8% for C19. Thus, the N6 and PET % mass values after $CaCO_3$ removal are closer to the true values.

After removing $CaCO_3$, PC4 was found to contain at least 3% but up to 15% total combined N6 and PET by mass (1-4% N6 and 2-11% PET). C17 had no measurable peaks for N6 or PET before $CaCO_3$ removal; however, small, broad peaks were observed and measured after $CaCO_3$ removal (1% N6 and 3% PET). Quantified plastic for sample B17 only decreased from 17% to 15%. On the other hand, sample C19, which had 18% total plastic in untreated PC4, dropped to just 8% total plastic after removing $CaCO_3$. This could be due to an amplification in peak height values due to the presence of $CaCO_3$ absorbance, especially for N6 which is close to the absorbance region for $CaCO_3$ (Figure 3).

µFTIR imaging and k-means clustering were useful in mapping key components of PC4: $CaCO_3$, N6, and PET as well as regions where multiple components are less easily distinguishable due to close spatial proximity (Figure 5). Maps of PC4 samples B17 and C19 (Supplementary Data Appendix, Figures 2 and 3) reveal chemical, physical, and spatial variations. Microplastic

particles in carpet powder have dimensions of at least 40 µm. We also identified material previously unidentified with our standard benchtop ATR-FTIR and bulk PC4. PS latex was identified in the bulk sample using µFTIR imaging without needing chemical removal of $CaCO_3$.

The content of PET in PC4 is of special concern due to the bioavailability of antimony (Sb) when PC4 was applied to soil in unpublished work from Dr. Peter Green (UC Davis Department of Civil and Environmental Engineering). For concrete made with PC4 replacing a portion of cement or fine aggregates, concentrations of Sb leached from concrete were below CA safety levels, however PC4 with elevated levels of PET fibers could cause higher concentrations of Sb leaching (Cunningham et al., 2021). Even after heat treatment, Sb content from PET presents a challenge in commercial use of PC4.

Heat Treatment of PC4

Heat treatment at 500 °C removed key spectral peaks used to quantify PET and N6. Qualitative analysis also revealed the presence of peaks likely associated with thermal decomposition products, particularly around 1500 cm^{-1} (Figures 6 and 7). Treatment at 600 and 680 °C removed all detectable peaks associated with plastics and the spectra closely match that of pure $CaCO_3$ (Figure 6). Thus, 600 °C is the minimum recommended temperature treatment for removing microplastics (N6, PET, PP and PS latex) from PC4.

After heating at 600 °C and chemically removing $CaCO_3$, spectra of ash and char reveal remaining absorbance between 1200 and 900cm^{-1} (Figures 7 and 8). C17 ash and C19 char contain particularly sharp peaks around 1200 cm^{-1} even after spectral subtraction of PTFE absorbance peaks from filter material in nearly the same wavenumber region. It is possible that these peaks are still coming from the PTFE filter although shifted in a way that impedes spectral

subtraction due to overlap with a wide absorbance band with a peak around 1000cm^{-1}. These peaks could be more prominent in these samples based on the thickness of sample deposited on the filters. C17 ash and C19 char do have a particularly thin layer of sample, visible from filter photos in Supplementary Data Appendix, Figure 4. Both C17 and C19 ash display a wide absorbance peak around 1000 cm^{-1} along with C19 char (no char sample available for C17). This peak may be attributed to the presence of quartz (Bosch-Reig et al., 2017), potentially from sand tracked in by foot traffic during carpet use which would not be eliminated by furnace treatment.

While sample B17 contains the fewest absorbance peaks after ashing, the char contrasts markedly with absorbance around 1000 cm^{-1} as well as around 1600 cm^{-1} (Figure 8). Absorbance around 1600 cm^{-1} indicates polyaromatic hydrocarbon groups or benzene ring structures which should be present in higher amounts in char than ash, where oxygen is not present to react. As for the absorbance around 1000 cm^{-1}, the presence of quartz would not be impacted by oxygen during furnace treatment, but a wide range of materials with reactive functional groups such as amines, alcohols, ethers, esters, carboxylic acids or anhydrides all display absorbance in the range of 1300 – 1000 cm^{-1} and alkenes display out-of-plane bending in the region from 1000-650 cm^{-1} (Pavia et al., 2015).

Although research in thermal treatment of sewage sludge for microplastic contamination suggests that a minumum pyrolysis temperature of 450 °C is sufficient for decomposing 99.7% of microplastic particles, our data shows that higher temperature, (600 °C) is necessary to remove PET and N6 (Ni et al., 2020). While PET and N6 were degraded at 500 °C, displaying FTIR absorbance peaks in similar but shifted locations compared to unheated PC4, plastic particles were not entirely decomposed (Figure 7). Our FTIR spectra did not suggest consistant

differences between heat treatments with or without oxygen, other research suggests charring (pyrolysis) without oxygen could be a better option since ashing or incinerating PC4 in the presence of oxygen could produce more harmful emissions such as furans and dioxins (Conesa et al., 2009).

Conclusions:

Tackling the challenge of plastic waste requires the development of better, more robust recycling methods for a wider array of products containing plastic, especially mixed materials such as carpet. While carpet recycling has increased in recent years, especially in CA, (Peoples, 2017), it has proved difficult to find customers for PC4, in contrast to the plastic fiber. Heat treatment for 1 hour at 600 °C with or without oxygen present could more safely allow for PC4's commercial use since it effectivley removes the combined mass % of PET and N6 from 15% down to less than 0.44%.

Use as agricultural soil amendment is still inadvisable due to Sb in PC4 that would not be mitigated by furnace treatment. Sb also presents challenges for PC4 use in concrete due to it's potential to leach over time, possibly at unafe concentrations since some PC4 samples contains more PET than others. Processing PET carpet separately from other carpets may be needed to mitigate Sb in PC4. While Sb from PET is a pernicious challenge, mechanical processing changes made at facility C yeilded a PC4 sample with much fewer visible plastic fibers as well as a shift form PP to PET and N6 microplastic. Adding thermal treatment at 600 °C would further cleanup PC4 in the interest of wider commercial appicability.

Although PET and N6 were quantified from ATR-FTIR spectra without any chemical removal of $CaCO_3$, the wide absorbance band for carbonate obscured the majority of PC4 contents. A solution of 2% HCl was highly effective in removing $CaCO_3$ below FTIR detection limits without presenting any changes in the spectra of PET and N6 standard microspheres. PS latex and PP also seemed to be uneffected by the dilute HCl treatment.

Our methods of μFTIR imaging could use additional refinement, but yielded maps that could be classified into clear regions containing PET and N6 as well as $CaCO_3$ using k-means clustering. Automated analysis of chemical imaging data is an exciting area of development in microplastics research. The development of accurate, precise, and crucially, cost-effective methods for routine analysis of microplastic in a wide variety of mediums is absolutely essential as concerns grow over potential toxicological concerns related to both microplastic and nanoplastic which are now globally ubiquitous.

This study presents unique applications of ATR-FTIR and μFTIR imaging for analyzing the microplastic content of post-consumer material from carpet recycling, PC4. This research can benefit the carpet recycling and manufacturing industries as well as CA state agencies of challenges surrounding post-consumer use of PC4 as well as possible solutions. While perfect mechanical separation between plastic fiber and $CaCO_3$ backing material is not possible, 600 °C heat treatment provides a cleaner final product and prevents microplastic from entering the environment. While the problem of environmental microplastic pollution is global in scale, all efforts to prevent additional inputs are a step in the right direction.

Future Research Directions:

While we developed calibration curves for N6 and PET in PC4 based on spectra of bulk sample containing $CaCO_3$, the chemical removal of $CaCO_3$ presented additional components, PP and PS latex for which quantification methods should be developed, potentially using a standard addition method as has been used in the context of, for example, quantification of bound styrene in its copolymers (P. Zhang et al., 2008)

Although we had difficulty collecting µFTIR images for individual particles without compressing sample underneath a Ge hemisphere, other studies have more successfully conducted reflectance-mode µFTIR imaging with an FPA detector and sample plastic fragments placed directly on a microscope slide (Tagg et al., 2015). Additional method could yield quantitative results from µFTIR using automated data analysis schemes developed by other researchers in promoting a more streamlined method with consistent standards for reporting microplastic data (Primpke et al., 2020).

Additional instrumentation such as liquid chromatography/mass spectrometry (LCMS) would provide a more detailed analysis of non-plastic components of PC4. Trace metals, especially Sb, and other organic chemicals such as PFAS and brominated flame retardants should be measured in unheated PC4 as well as ash and char. Unpublished data from Dr. Peter Green (UCD Department of Civil and Environmental Engineering) shows PC4 contains brominated flame retardants as well as perfluorinated compounds that are removed via furnace treatment. Based on instrument sensitivity, heat treatment removes >99% of brominated flame retardants analyzed and >80% removal for perfluorinated compounds.

Beyond analytical techniques, it would be useful to consider Life Cycle Assessment for $CaCO_3$ from PC4 compared to mining pure material. Carpet manufacturing is based nearby $CaCO_3$ mining operations while post-consumer PC4 would need transportation across hundreds to thousands of miles from CA to reach re-use in carpet manufacturing, based primarily in Dalton, GA. However, other uses for PC4 could reduce greenhouse gas emissions by reducing reliance on mining and transportation of fresh $CaCO_3$. Initial life cycle assessment for concrete with unheated PC4 used as an additive shows that significant greenhouse gas emissions reduction can be achieved proportional to the amount of PC4 used as a replacement for Portland cement (Cunningham et al., 2021).

References:

Anjos, O., Campos, M. G., Ruiz, P. C., & Antunes, P. (2015). Application of FTIR-ATR spectroscopy to the quantification of sugar in honey. *Food Chemistry*, *169*, 218–223. https://doi.org/10.1016/j.foodchem.2014.07.138

Bancin, L. J., Walther, B. A., Lee, Y.-C., & Kunz, A. (2019). Two-dimensional distribution and abundance of micro- and mesoplastic pollution in the surface sediment of Xialiao Beach, New Taipei City, Taiwan. *Marine Pollution Bulletin*, *140*, 75–85. https://doi.org/10.1016/j.marpolbul.2019.01.028

Bläsing, M., & Amelung, W. (2018). Plastics in soil: Analytical methods and possible sources. *Science of The Total Environment*, *612*, 422–435. https://doi.org/10.1016/j.scitotenv.2017.08.086

Bosch-Reig, F., Gimeno-Adelantado, J. V., Bosch-Mossi, F., & Doménech-Carbó, A. (2017). Quantification of minerals from ATR-FTIR spectra with spectral interferences using the MRC method. *Spectrochimica Acta Part A: Molecular and Biomolecular Spectroscopy*, *181*, 7–12. https://doi.org/10.1016/j.saa.2017.02.012

Brennecke, D., Duarte, B., Paiva, F., Caçador, I., & Canning-Clode, J. (2016). Microplastics as vector for heavy metal contamination from the marine environment. *Estuarine, Coastal and Shelf Science*, *178*, 189–195. https://doi.org/10.1016/j.ecss.2015.12.003

Browne, M. A., Galloway, T. S., & Thompson, R. C. (2010). Spatial Patterns of Plastic Debris along Estuarine Shorelines. *Environmental Science & Technology*, *44*(9), 3404–3409. https://doi.org/10.1021/es903784e

Cabernard, L., Roscher, L., Lorenz, C., Gerdts, G., & Primpke, S. (2018). Comparison of Raman and Fourier Transform Infrared Spectroscopy for the Quantification of Microplastics in the Aquatic Environment. *Environmental Science & Technology*, *52*(22), 13279–13288. https://doi.org/10.1021/acs.est.8b03438

Cai, L., Wang, J., Peng, J., Tan, Z., Zhan, Z., Tan, X., & Chen, Q. (2017). Characteristic of microplastics in the atmospheric fallout from Dongguan city, China: Preliminary research and first evidence. *Environmental Science and Pollution Research*, *24*(32), 24928–24935. https://doi.org/10.1007/s11356-017-0116-x

CARE 2017 Annual Report. (2018). Carpet America Recovery Effort. https://carpetrecovery.org/resources/annual-reports/

Carpenter, E. J., & Smith, K. L. (1972). Plastics on the Sargasso Sea Surface. *Science*, *175*(4027), 1240–1241. https://doi.org/10.1126/science.175.4027.1240

Carvalho, M. C. S., & van Raij, B. (1997). Calcium sulphate, phosphogypsum and calcium carbonate in the amelioration of acid subsoils for root growth. *Plant and Soil*, *192*(1), 37–48. https://doi.org/10.1023/A:1004285113189

Chen, Y., Furmann, A., Mastalerz, M., & Schimmelmann, A. (2014). Quantitative analysis of shales by KBr-FTIR and micro-FTIR. *Fuel*, *116*, 538–549. https://doi.org/10.1016/j.fuel.2013.08.052

Conesa, J. A., Font, R., Fullana, A., Martín-Gullón, I., Aracil, I., Gálvez, A., Moltó, J., & Gómez-Rico, M. F. (2009). Comparison between emissions from the pyrolysis and combustion of different wastes. *Journal of Analytical and Applied Pyrolysis*, *84*(1), 95–102. https://doi.org/10.1016/j.jaap.2008.11.022

Corami, F., Rosso, B., Bravo, B., Gambaro, A., & Barbante, C. (2020). A novel method for purification, quantitative analysis and characterization of microplastic fibers using Micro-FTIR. *Chemosphere*, *238*, 124564. https://doi.org/10.1016/j.chemosphere.2019.124564

Corradini, F., Meza, P., Eguiluz, R., Casado, F., Huerta-Lwanga, E., & Geissen, V. (2019). Evidence of microplastic accumulation in agricultural soils from sewage sludge disposal. *Science of The Total Environment*, *671*, 411–420. https://doi.org/10.1016/j.scitotenv.2019.03.368

Cunningham, P. R., Green, P. G., & Miller, S. A. (2021). Utilization of post-consumer carpet calcium carbonate (PC4) from carpet recycling as a material resource in concrete. *Resources, Conservation and Recycling*, *169*.

de Souza Machado, A. A., Horton, A. A., Davis, T., & Maaß, S. (2020). Microplastics and Their Effects on Soil Function as a Life-Supporting System. In D. He & Y. Luo (Eds.), *Microplastics in Terrestrial Environments: Emerging Contaminants and Major Challenges* (pp. 199–222). Springer International Publishing. https://doi.org/10.1007/698_2020_450

de Souza Machado, A. A., Kloas, W., Zarfl, C., Hempel, S., & Rillig, M. C. (2018). Microplastics as an emerging threat to terrestrial ecosystems. *Global Change Biology*, *24*(4), 1405–1416. https://doi.org/10.1111/gcb.14020

de Souza Machado, A. A., Lau, C. W., Kloas, W., Bergmann, J., Bachelier, J. B., Faltin, E., Becker, R., Görlich, A. S., & Rillig, M. C. (2019). Microplastics Can Change Soil Properties and Affect Plant Performance. *Environmental Science & Technology*, *53*(10), 6044–6052. https://doi.org/10.1021/acs.est.9b01339

ECHA. (2019). *Annex XV Restriction Report Proposal for a Restriction—Substance Name(s): Intentionally added microplastics*. European Chemicals Agency.

Enders, K., Lenz, R., Stedmon, C. A., & Nielsen, T. G. (2015). Abundance, size and polymer composition of marine microplastics ≥10μm in the Atlantic Ocean and their modelled vertical distribution. *Marine Pollution Bulletin*, *100*(1), 70–81. https://doi.org/10.1016/j.marpolbul.2015.09.027

European Union. (2017, May 17). *Commission Decision (EU) 2017/848 of 17 May 2017—Laying down criteria and methodological standards on good environmental status of marine waters and specifications and standardised methods for monitoring and assessment, and repealing Decision 2010/477/EU* [Website]. Publications Office of the European Union. http://op.europa.eu/en/publication-detail/-/publication/a7523a58-3b91-11e7-a08e-01aa75ed71a1/language-en

Faltynkova, A., Johnsen, G., & Wagner, M. (2021). Hyperspectral imaging as an emerging tool to analyze microplastics: A systematic review and recommendations for future development. *Microplastics and Nanoplastics*, *1*(1), 13. https://doi.org/10.1186/s43591-021-00014-y

Fischer, M., & Scholz-Böttcher, B. M. (2017). Simultaneous Trace Identification and Quantification of Common Types of Microplastics in Environmental Samples by Pyrolysis-Gas Chromatography–Mass Spectrometry. *Environmental Science & Technology*, *51*(9), 5052–5060. https://doi.org/10.1021/acs.est.6b06362

Fuller, S., & Gautam, A. (2016). A Procedure for Measuring Microplastics using Pressurized Fluid Extraction. *Environmental Science & Technology*, *50*(11), 5774–5780. https://doi.org/10.1021/acs.est.6b00816

Gaston, E., Woo, M., Steele, C., Sukumaran, S., & Anderson, S. (2020). Microplastics Differ Between Indoor and Outdoor Air Masses: Insights from Multiple Microscopy Methodologies. *Applied Spectroscopy*, *74*(9), 1079–1098.

Gelardi, D. L., & Parikh, S. J. (2021). Soils and Beyond: Optimizing Sustainability Opportunities for Biochar. *Sustainability*, *13*(18), 10079. https://doi.org/10.3390/su131810079

Geyer, R. (2020). Chapter 2—Production, use, and fate of synthetic polymers. In T. M. Letcher (Ed.), *Plastic Waste and Recycling* (pp. 13–32). Academic Press. https://doi.org/10.1016/B978-0-12-817880-5.00002-5

Geyer, R., Jambeck, J. R., & Law, K. L. (2017). Production, use, and fate of all plastics ever made. *Science Advances*, *3*(7), e1700782. https://doi.org/10.1126/sciadv.1700782

Hao, Z., Bechtel, H. A., Kneafsey, T., Gilbert, B., & Nico, P. S. (2018). Cross-Scale Molecular Analysis of Chemical Heterogeneity in Shale Rocks. *Scientific Reports*, *8*(1), 2552. https://doi.org/10.1038/s41598-018-20365-6

Harrison, J. P., Ojeda, J. J., & Romero-González, M. E. (2012). The applicability of reflectance micro-Fourier-transform infrared spectroscopy for the detection of synthetic microplastics in marine sediments. *Science of The Total Environment*, *416*, 455–463. https://doi.org/10.1016/j.scitotenv.2011.11.078

He, D., Luo, Y., Lu, S., Liu, M., Song, Y., & Lei, L. (2018). Microplastics in soils: Analytical methods, pollution characteristics and ecological risks. *TrAC Trends in Analytical Chemistry*, *109*, 163–172. https://doi.org/10.1016/j.trac.2018.10.006

Henry, D. G., Watson, J. S., & John, C. M. (2017). Assessing and calibrating the ATR-FTIR approach as a carbonate rock characterization tool. *Sedimentary Geology*, *347*, 36–52. https://doi.org/10.1016/j.sedgeo.2016.07.003

Hidalgo-Ruz, V., Gutow, L., Thompson, R. C., & Thiel, M. (2012). Microplastics in the Marine Environment: A Review of the Methods Used for Identification and Quantification. *Environmental Science & Technology*, *46*(6), 3060–3075. https://doi.org/10.1021/es2031505

Huppertsberg, S., & Knepper, T. P. (2018). Instrumental analysis of microplastics—Benefits and challenges. *Analytical and Bioanalytical Chemistry*, *410*(25), 6343–6352. https://doi.org/10.1007/s00216-018-1210-8

Ivleva, N. P. (2021). Chemical Analysis of Microplastics and Nanoplastics: Challenges, Advanced Methods, and Perspectives. *Chemical Reviews*, *121*(19), 11886–11936. https://doi.org/10.1021/acs.chemrev.1c00178

Käppler, A., Fischer, D., Oberbeckmann, S., Schernewski, G., Labrenz, M., Eichhorn, K.-J., & Voit, B. (2016). Analysis of environmental microplastics by vibrational microspectroscopy: FTIR, Raman or both? *Analytical and Bioanalytical Chemistry*, *408*(29), 8377–8391. https://doi.org/10.1007/s00216-016-9956-3

Kunz, A., Walther, B. A., Löwemark, L., & Lee, Y.-C. (2016). Distribution and quantity of microplastic on sandy beaches along the northern coast of Taiwan. *Marine Pollution Bulletin*, *111*(1), 126–135. https://doi.org/10.1016/j.marpolbul.2016.07.022

Lenz, R., Enders, K., Stedmon, C. A., Mackenzie, D. M. A., & Nielsen, T. G. (2015). A critical assessment of visual identification of marine microplastic using Raman spectroscopy for analysis improvement. *Marine Pollution Bulletin*, *100*(1), 82–91. https://doi.org/10.1016/j.marpolbul.2015.09.026

Li, J., Zhang, K., & Zhang, H. (2018). Adsorption of antibiotics on microplastics. *Environmental Pollution*, *237*, 460–467. https://doi.org/10.1016/j.envpol.2018.02.050

Lin, H., Bean, S. R., Tilley, M., Peiris, K. H. S., & Brabec, D. (2021). Qualitative and Quantitative Analysis of Sorghum Grain Composition Including Protein and Tannins Using ATR-FTIR Spectroscopy. *Food Analytical Methods*, *14*(2), 268–279. https://doi.org/10.1007/s12161-020-01874-5

Löder, M. G. J., Kuczera, M., Mintenig, S., Lorenz, C., & Gerdts, G. (2015). Focal plane array detector-based micro-Fourier-transform infrared imaging for the analysis of microplastics in environmental samples. *Environmental Chemistry*, *12*(5), 563–581. https://doi.org/10.1071/EN14205

Mahon, A. M., O'Connell, B., Healy, M. G., O'Connor, I., Officer, R., Nash, R., & Morrison, L. (2017). Microplastics in Sewage Sludge: Effects of Treatment. *Environmental Science & Technology*, *51*(2), 810–818. https://doi.org/10.1021/acs.est.6b04048

Moschet, C., Anumol, T., Lew, B. M., Bennett, D. H., & Young, T. M. (2018). Household Dust as a Repository of Chemical Accumulation: New Insights from a Comprehensive High-Resolution Mass Spectrometric Study. *Environmental Science & Technology*, *52*(5), 2878–2887. https://doi.org/10.1021/acs.est.7b05767

Mukome, F. N. D., Zhang, X., Silva, L. C. R., Six, J., & Parikh, S. J. (2013). Use of Chemical and Physical Characteristics To Investigate Trends in Biochar Feedstocks. *Journal of Agricultural and Food Chemistry*, *61*(9), 2196–2204. https://doi.org/10.1021/jf3049142

Ni, B.-J., Zhu, Z.-R., Li, W.-H., Yan, X., Wei, W., Xu, Q., Xia, Z., Dai, X., & Sun, J. (2020). Microplastics Mitigation in Sewage Sludge through Pyrolysis: The Role of Pyrolysis Temperature. *Environmental Science & Technology Letters*, *7*(12), 961–967. https://doi.org/10.1021/acs.estlett.0c00740

Nizzetto, L., Langaas, S., & Futter, M. (2016). Pollution: Do microplastics spill on to farm soils? *Nature*, *537*(7621), 488–488. https://doi.org/10.1038/537488b

Nuelle, M.-T., Dekiff, J. H., Remy, D., & Fries, E. (2014). A new analytical approach for monitoring microplastics in marine sediments. *Environmental Pollution*, *184*, 161–169. https://doi.org/10.1016/j.envpol.2013.07.027

Pavia, D. L., Lampman, G. M., Kriz, G. S., & Vyvyan, J. R. (2015). *Introduction to Spectroscopy* (5th ed.). Cengage.

Peoples, R. (2017). *Californial Carpet Stewardship Plan 2017-2021*. Carpet America Recovery Effort. https://www.calrecycle.ca.gov/Carpet/Plans/

Peoples, R. (2018). *California Carpet Stewardship Plan 2018—2022*. Carpet America Recovery Effort. https://www.calrecycle.ca.gov/Carpet/Plans/

Product stewardship: Carpet, AB 2398, 30 Public Resources (2010). https://carpetrecovery.org/california/california-ab-2398/#law

California Safe Drinking Water Act: Microplastics, 1422, Senate, Health and Safety (2018). https://leginfo.legislature.ca.gov/faces/billTextClient.xhtml?bill_id=201720180SB1422

Ocean Protection Council: Statewide Microplastics Strategy, 1263, Senate, 26.5 Public Resources (2018). https://legiscan.com/CA/text/SB1263/id/1820639

Primpke, S., Christiansen, S. H., Christiansen, S. H., Christiansen, S. H., Cowger, W., Frond, H. D., Deshpande, A., Fischer, M., Holland, E. B., Meyns, M., O'Donnell, B. A., Ossmann, B. E., Ossmann, B. E., Pittroff, M., Sarau, G., Sarau, G., Scholz-Böttcher, B. M., & Wiggin, K. J. (2020). Critical Assessment of Analytical Methods for the Harmonized and Cost-Efficient Analysis of Microplastics. *Applied Spectroscopy*, *74*(9), 1012–1047.

Rainieri, S., & Barranco, A. (2019). Microplastics, a food safety issue? *Trends in Food Science & Technology*, *84*, 55–57. https://doi.org/10.1016/j.tifs.2018.12.009

Rillig, M. C. (2012). Microplastic in Terrestrial Ecosystems and the Soil? *Environmental Science & Technology*, *46*(12), 6453–6454. https://doi.org/10.1021/es302011r

Rillig, M. C. (2018). Microplastic Disguising As Soil Carbon Storage. *Environmental Science & Technology*, *52*(11), 6079–6080. https://doi.org/10.1021/acs.est.8b02338

Rocha-Santos, T. A. P., & Duarte, A. C. (2017). *Characterization and Analysis of Microplastics* (Vol. 75).

Royer, S.-J., Ferrón, S., Wilson, S. T., & Karl, D. M. (2018). Production of methane and ethylene from plastic in the environment. *PLOS ONE*, *13*(8), e0200574. https://doi.org/10.1371/journal.pone.0200574

Schecter, A., Päpke, O., Joseph, J. E., & Tung, K.-C. (2005). Polybrominated Diphenyl Ethers (PBDEs) In U.S. Computers and Domestic Carpet Vacuuming: Possible Sources of Human Exposure. *Journal of Toxicology and Environmental Health, Part A*, *68*(7), 501–513. https://doi.org/10.1080/15287390590909715

Scheurer, M., & Bigalke, M. (2018). Microplastics in Swiss Floodplain Soils. *Environmental Science & Technology*, *52*(6), 3591–3598. https://doi.org/10.1021/acs.est.7b06003

Schreiber, M. J., & Nunez, G. H. (2021). Calcium Carbonate Can Be Used to Manage Soilless Substrate pH for Blueberry Production. *Horticulturae*, *7*(4), 74. https://doi.org/10.3390/horticulturae7040074

Shan, J., Zhao, J., Liu, L., Zhang, Y., Wang, X., & Wu, F. (2018). A novel way to rapidly monitor microplastics in soil by hyperspectral imaging technology and chemometrics. *Environmental Pollution*, *238*, 121–129. https://doi.org/10.1016/j.envpol.2018.03.026

Shan, J., Zhao, J., Zhang, Y., Liu, L., Wu, F., & Wang, X. (2019). *Simple and rapid detection of microplastics in seawater using hyperspectral imaging technology*. https://www.sciencedirect.com/science/article/pii/S0003267018313461

Shim, W. J., Hong, S. H., & Eo, S. E. (2017a). Identification methods in microplastic analysis: A review. *Analytical Methods*, *9*(9), 1384–1391. https://doi.org/10.1039/C6AY02558G

Shim, W. J., Hong, S. H., & Eo, S. E. (2017b). Identification methods in microplastic analysis: A review. *Analytical Methods*, *9*(9), 1384–1391. https://doi.org/10.1039/C6AY02558G

Silva, A. B., Bastos, A. S., Justino, C. I. L., da Costa, J. P., Duarte, A. C., & Rocha-Santos, T. A. P. (2018). Microplastics in the environment: Challenges in analytical chemistry - A review. *Analytica Chimica Acta*, *1017*, 1–19. https://doi.org/10.1016/j.aca.2018.02.043

Song, Y. K., Hong, S. H., Jang, M., Han, G. M., Rani, M., Lee, J., & Shim, W. J. (2015). A comparison of microscopic and spectroscopic identification methods for analysis of microplastics in environmental samples. *Marine Pollution Bulletin*, *93*(1), 202–209. https://doi.org/10.1016/j.marpolbul.2015.01.015

Sotayo, A., Green, S., & Turvey, G. (2015). Carpet recycling: A review of recycled carpets for structural composites. *Environmental Technology & Innovation*, *3*, 97–107. https://doi.org/10.1016/j.eti.2015.02.004

Tagg, A. S., Sapp, M., Harrison, J. P., & Ojeda, J. J. (2015). Identification and Quantification of Microplastics in Wastewater Using Focal Plane Array-Based Reflectance Micro-FT-IR Imaging. *Analytical Chemistry*, *87*(12), 6032–6040. https://doi.org/10.1021/acs.analchem.5b00495

Teuten, E. L., Rowland, S. J., Galloway, T. S., & Thompson, R. C. (2007). Potential for Plastics to Transport Hydrophobic Contaminants. *Environmental Science & Technology*, *41*(22), 7759–7764. https://doi.org/10.1021/es071737s

Thompson, R. C., Olsen, Y., Mitchell, R. P., Davis, A., & al, et. (2004). Lost at Sea: Where Is All the Plastic? *Science*, *304*(5672), 838.

UNEP. (2016). *Marine Plastic Debris & Microplastics—Global Lessons and Reserach to Inspire Action and Guide Policy Change*. United Nations Environment Programme.

United Nations. (n.d.). *Transforming our World: The 2030 Agenda for Sustainable Development*. Retrieved October 7, 2021, from https://sdgs.un.org/publications/transforming-our-world-2030-agenda-sustainable-development-17981

US EPA, O. (2020). *National Overview: Facts and Figures on Materials, Wastes and Recycling* [Overviews and Factsheets]. https://www.epa.gov/facts-and-figures-about-materials-waste-and-recycling/national-overview-facts-and-figures-materials

Vianello, A., Boldrin, A., Guerriero, P., Moschino, V., Rella, R., Sturaro, A., & Da Ros, L. (2013). Microplastic particles in sediments of Lagoon of Venice, Italy: First observations on occurrence, spatial patterns and identification. *Estuarine, Coastal and Shelf Science*, *130*, 54–61. https://doi.org/10.1016/j.ecss.2013.03.022

Walker, T. R. (2021). (Micro)plastics and the UN Sustainable Development Goals. *Current Opinion in Green and Sustainable Chemistry*, *30*, 100497. https://doi.org/10.1016/j.cogsc.2021.100497

Wang, J., Liu, X., Li, Y., Powell, T., Wang, X., Wang, G., & Zhang, P. (2019). Microplastics as contaminants in the soil environment: A mini-review. *Science of The Total Environment*, *691*, 848–857. https://doi.org/10.1016/j.scitotenv.2019.07.209

Wong, C. S., Green, D. R., & Cretney, W. J. (1974). Quantitative Tar and Plastic Waste Distributions in the Pacific Ocean. *Nature*, *247*(5435), 30–32. https://doi.org/10.1038/247030a0

Zhang, P., He, J., & Zhou, X. (2008). An FTIR standard addition method for quantification of bound styrene in its copolymers. *Polymer Testing*, *27*(2), 153–157. https://doi.org/10.1016/j.polymertesting.2007.09.004

Zhang, Y., Wang, X., Shan, J., Zhao, J., Zhang, W., Liu, L., & Wu, F. (2019). Hyperspectral Imaging Based Method for Rapid Detection of Microplastics in the Intestinal Tracts of Fish. *Environmental Science & Technology*, *53*(9), 5151–5158. https://doi.org/10.1021/acs.est.8b07321

Zhou, Q., Zhang, H., Fu, C., Zhou, Y., Dai, Z., Li, Y., Tu, C., & Luo, Y. (2018). The distribution and morphology of microplastics in coastal soils adjacent to the Bohai Sea and the Yellow Sea. *Geoderma*, *322*, 201–208. https://doi.org/10.1016/j.geoderma.2018.02.015

Zhu, Y., Ro, A., & Bartell, S. M. (2021). Household low pile carpet usage was associated with increased serum PFAS concentrations in 2005–2006. *Environmental Research*, *195*, 110758. https://doi.org/10.1016/j.envres.2021.110758

Supplementary Data Appendix

Table 1: Summary of heat treatment parameters for PC4 ash and char samples.

Sample	Preheat Time (hr)	Hold Time (hr)	Hold Temp Range (°C)	Reported Temp. (°C)
B17, C17	1.5	1	480 - 500	500
B17, C17	5	1	580 - 600	600
B17, C17	5.5	0.5	640 - 650	650
B17, C17	8	2.5	660 - 680	680
C19	4	1	580 - 620	600
C19	3	1.5	560 - 600	600
C19	3	1	580 - 610	600
B17, C19	4.5	1	590 - 600	600
B17, C19	*4	*1	*580 - 600	600

*This treatment excluded oxygen (char, not ash).

Table 2: Explained variance for PCA and silhouette scores for k-Means clustering to summarize effectiveness of PCA and k-Means for our data when choosing 2-4 components for each map collected for samples B17 and C19. The highest value is shaded for each map.

	PCA explained variance % (2-4 components)			k-Means Silhouette Scores (2-4 components)		
Map	**2**	**3**	**4**	**2**	**3**	**4**
B17 (0)	46%	53%	57%	0.272	0.293	0.27
B17 (1)	60%	77%	84%	0.33	0.389	0.445
C19 (1)	56%	64%	66%	0.337	0.381	0.38
C19 (2)	65%	77%	81%	0.652	0.294	0.231
C19 (3)	81%	86%	89%	0.458	0.372	0.382
C19 (4)	71%	79%	84%	0.352	0.237	0.216
C19 (5)	65%	80%	85%	0.433	0.451	0.489
C19 (6)	82%	87%	90%	0.55	0.493	0.473

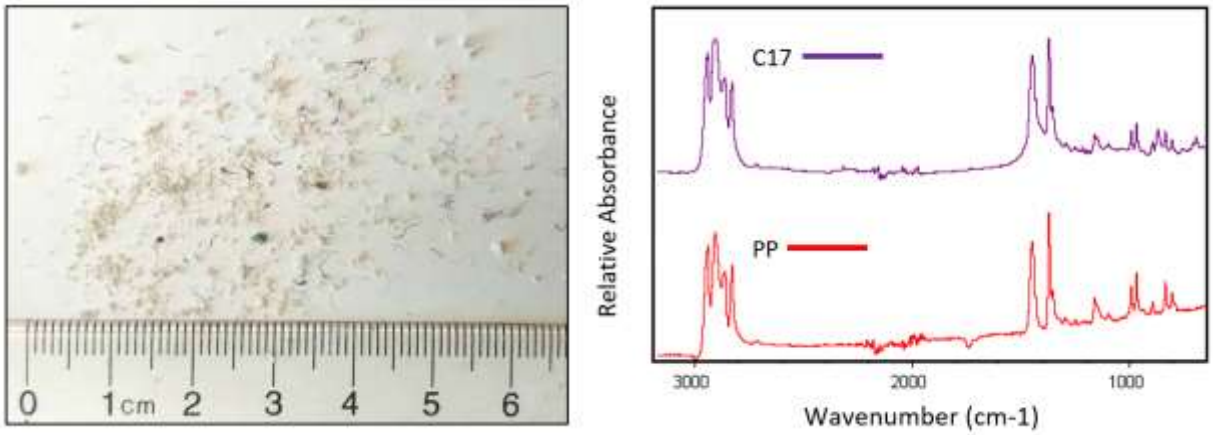

Figure 1: Photo of PC4 sample C17 along with ATR-FTIR spectra of sample C17 and a polypropylene (PP) standard. Photo credit: Alice Henderson.

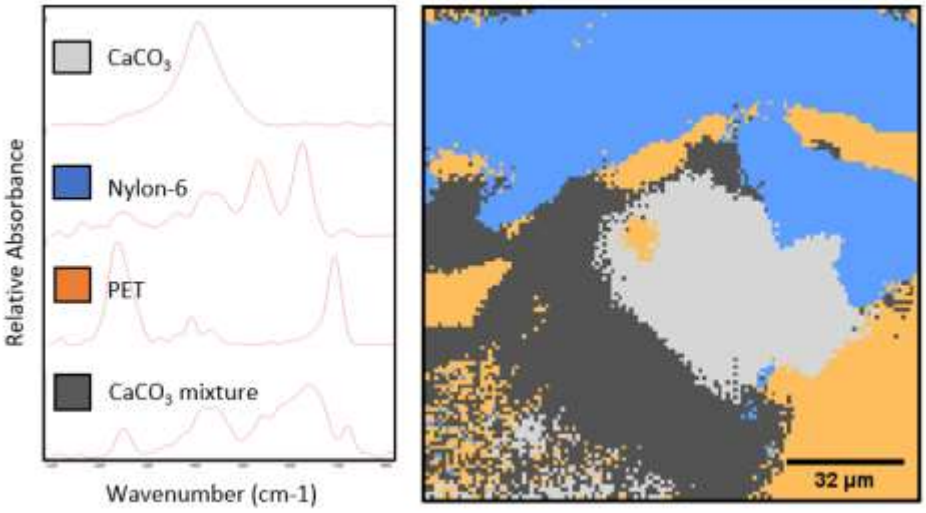

Figure 2: Representative spectra from each component identified via k-means clustering alongside a reconstructed image colored based on k-means clustering for unheated PC4 sample B17. The example spectra show typical features for the pixels of the color indicated.

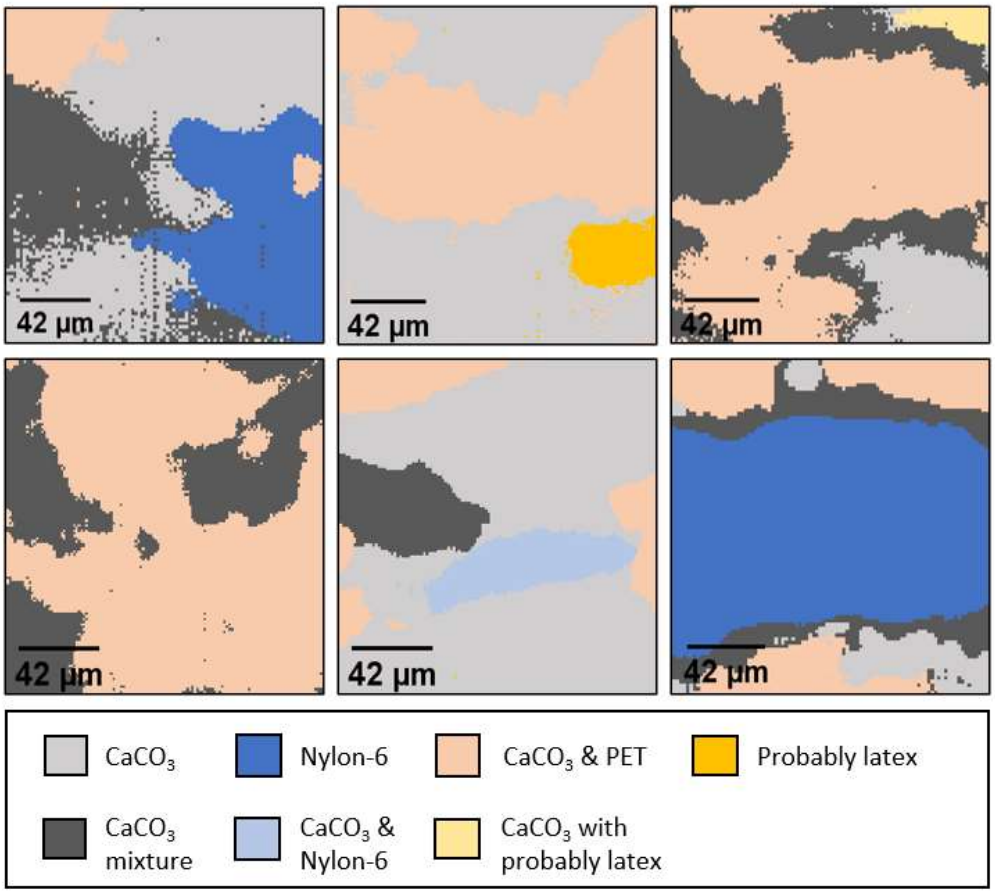

Figure 3: Reconstructed images from the unheated PC4 sample, C19, colored based on k-means clustering and described in the legend by comparing FTIR spectra to standards known or suspected to be present in PC4.

Table 3: Mass loss data for six samples during the initial 600 °C treatment of five size fractions of PC4 sample C17, and bulk samples B17 and C19.

Sample	Temperature Treatment	Mass Loss (%)
B17	500 °C, 1hr	25
	600 °C, 1hr	32
	680 °C, 1hr	35
C17	500 °C, 1hr	18
	600 °C, 1hr	21
	680 °C, 1hr	22
C19	600 °C, 1hr	22

Table 4: Percent mass remaining after chemically removing CaCO3 from samples of PC4 compared with percent mass lost from combusting or pyrolyzing PC4 samples at 600 °C. These values approximate the amount of plastic and organic content in PC4.

Sample	%mass remaining after HCl	% mass lost at 600 °C
B17	27	32
B17 ash 500	15	
B17 ash 600	9	
B17 char 600	10	
C17	15	21
C17 ash 500	3	
C17 ash 600	2	
C19	18	22
C19 ash 600	4	
C19 char 600	4	
CaCO3	0	

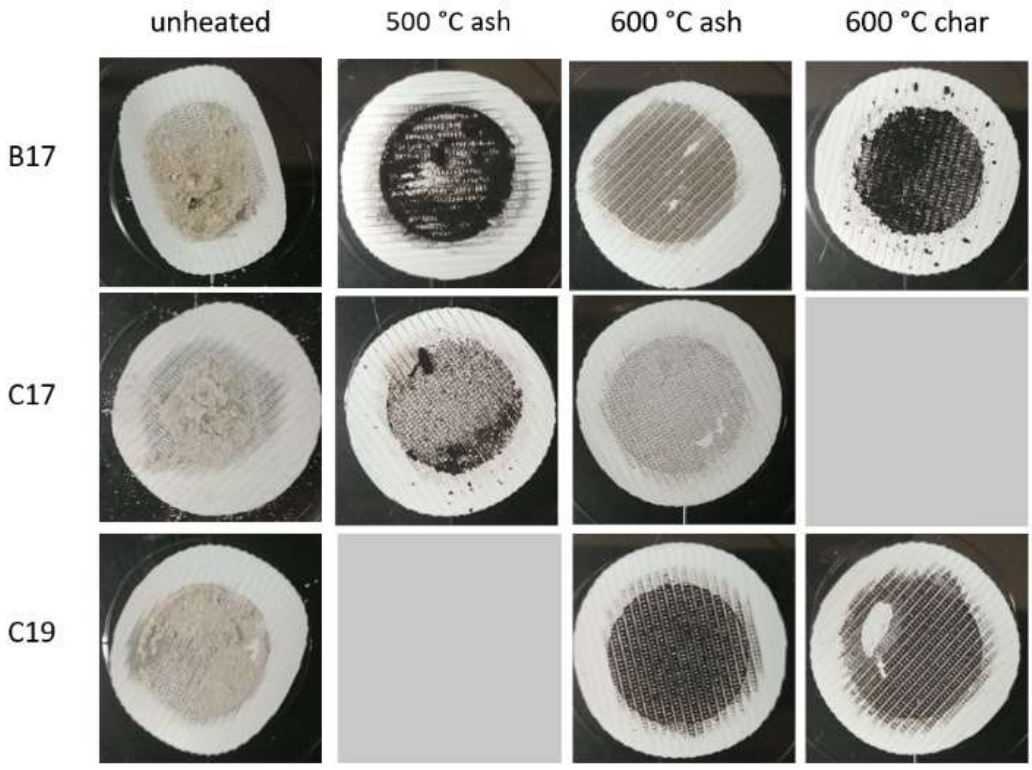

Figure 4: Photos of 25 mm, PTFE membrane filters with concentrated non-$CaCO_3$ components of PC4, unheated as well as ashed and charred. Photo credit: Alice Henderson.